Thermodynamic and optical properties of $NdCr_3(BO_3)_4$

E. A. Popova* and N. I. Leonyuk
Moscow State University, 119992 Moscow, Russia

M. N. Popova, E. P. Chukalina, and K. N. Boldyrev
Institute of Spectroscopy, RAS, 142190 Troitsk, Moscow, Russia

N. Tristan, R. Klingeler, and B. Büchner
Leibniz-Institute for Solid State and Materials Research, IFW, Dresden, 01171 Dresden, Germany
(Received 18 April 2007; revised manuscript received 19 June 2007; published 27 August 2007)

We present magnetization and specific heat data as well as optical spectra of $NdCr_3(BO_3)_4$ single crystals. At $T_N=8$ K, the magnetic and specific heat data imply long-range antiferromagnetic spin order of the Cr^{3+} subsystem. This observation is corroborated by the spectroscopic studies since in the ordered state the Nd^{3+} Kramers doublets are split by the internal staggered magnetic field. The splitting is also visible in a Schottky anomaly at the specific heat. In the spin-ordered phase, we find a staggered magnetic field at the Nd sites of 35 kG at 1.8 K. The values $\lambda_{Nd\text{-}Cr}=3.9$ kG/μ_B and $\lambda_{Cr\text{-}Cr}=29.4$ kG/μ_B are obtained for the molecular-field constants of the Nd-Cr and the Cr-Cr interactions, respectively. The analysis of the magnetic susceptibility data points to the easy-plane type of the antiferromagnetic order. Several experimental manifestations of the low dimensionality of the title compound are mentioned.

DOI: 10.1103/PhysRevB.76.054446 PACS number(s): 75.30.−m, 75.40.Cx, 78.30.−j, 71.70.Ch

I. INTRODUCTION

Borates with the general formula $RM_3(BO_3)_4$ (R=Y,La-Lu; M=Al,Ga,Sc,Fe,Cr) have a trigonal structure of the natural mineral huntite $CaMg_3(CO_3)_4$ (see, e.g., Ref. 1). Aluminates from this family have attracted a considerable attention because of their good luminescent and nonlinear optical properties[2] combined with high mechanical strength, good thermal and chemical stability, and beam resistance. In 1981 it was suggested to use the $YAl_3(BO_3)_4$:Nd crystals for self-frequency-doubling lasers.[3] Since then, different self-frequency-doubling and self-frequency-summing lasers were developed on the basis of Nd-doped $YAl_3(BO_3)_4$ and $GdAl_3(BO_3)_4$ crystals (see, e.g., Refs. 4 and 5, and references therein). Concentrated crystals $NdAl_3(BO_3)_4$ are efficient media for minilasers.[6] In contrast, the borates with magnetic ions (M=Fe,Cr) have been much less investigated. Recent studies of rare-earth iron borates $RFe_3(BO_3)_4$ have shown that these compounds exhibit a variety of phase transitions. Their magnetic properties are governed by the presence of two interacting magnetic subsystems, i.e., the Fe^{3+} and the R^{3+} moments. It turns out that the magnetic structure of $RFe_3(BO_3)_4$ changes as a function of temperature, external magnetic field, and substitutions in the rare-earth subsystem.[7–11] Interestingly, at least two compounds belonging to the family of rare-earth iron borates, namely $GdFe_3(BO_3)_4$ and $NdFe_3(BO_3)_4$, display a considerable magnetoelectric coupling and their electric (magnetic) properties can be controlled by the magnetic (electric) field.[12–14] This is a promising finding in view of possible device applications. It is worth mentioning that $NdFe_3(BO_3)_4$, exhibits a much stronger magnetoelectric coupling than $GdFe_3(BO_3)_4$.[13]

Up to now, only little is known about the properties of the rare-earth borates $RCr_3(BO_3)_4$ with another magnetic ion, i.e., chromium. x-ray diffraction studies at room temperature have established the huntite-type trigonal structure with the space group $R32$ for powder samples of $GdCr_3(BO_3)_4$ (Ref. 15) and for small single crystals of $RCr_3(BO_3)_4$, R=Nd, Sm, Eu, Gd, Tb, Ho, and Yb.[1] The main elements of the structure are spiral chains of edge-sharing CrO_6 octahedra running along the c axis. RO_6 prisms and two kinds of BO_3 triangles connect three CrO_6 chains. The only study on $RCr_3(BO_3)_4$ which addressed other than structural properties concerned the room-temperature absorption and luminescence spectra of $NdCr_3(BO_3)_4$ single crystals.[16] In order to understand the magnetic properties of this compound we hence present data on the magnetic, thermodynamic, and optical properties of a $NdCr_3(BO_3)_4$ single crystal in a wide range of temperature.

II. EXPERIMENT

Single crystals of $NdCr_3(BO_3)_4$ were obtained by spontaneous nucleation from the K_2SO_4-$3MoO_3$ and $K_2Mo_3O_{10}$-based fluxes at cooling rate 2–3 °C/hour in the temperature range 1150 °C–900 °C. The single crystals of $NdCr_3(BO_3)_4$ were coal black with blue tint. The size of the crystals was less than 1 mm^3. The x-ray analysis confirmed their $R32$ structure at room temperature with the hexagonal crystal lattice parameters $a=9.487(2)$ and $c=7.497(2)$ Å.[1] For specific heat and magnetic measurements, several small pieces of the same batch were put together by Apiezon grease. The high fragility of the crystals made their cutting and polishing practically impossible. Therefore, the measurements were carried out on nonoriented samples and thin as-grown crystals were used for the optical measurements.

Magnetization measurements were performed in the temperature range 1.75–350 K in magnetic fields up to 50 kG using a Quantum Design SQUID magnetometer. The heat capacity was measured in the temperature range 0.4–300 K

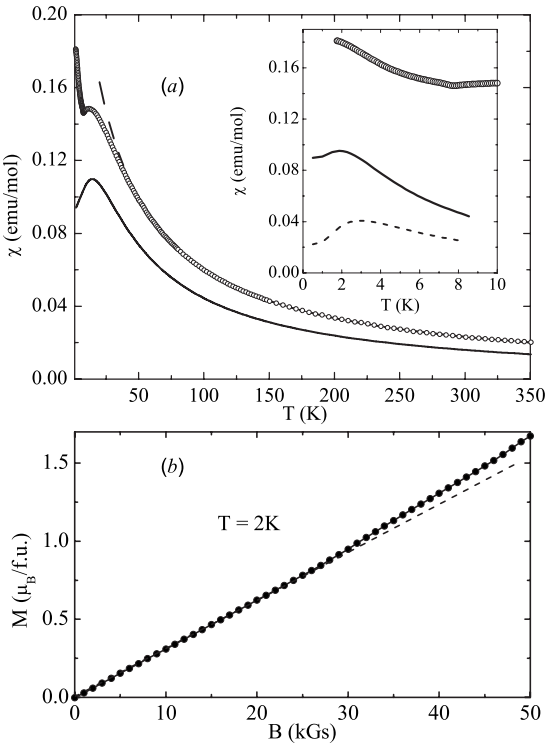

FIG. 1. (a) Temperature dependence of the magnetic susceptibility $\chi(T)$ of $NdCr_3(BO_3)_4$ measured in the magnetic field 1 kG (open circles). The dashed line corresponds to the Curie-Weiss law. The solid line shows the magnetic susceptibility of the $s=3/2$ spin chain calculated by means of Eq. (7) with the value of the intrachain exchange parameter $J=4$ K. The inset displays the low-temperature part of $\chi(T)$, together with the calculated (solid and dashed lines) paramagnetic contribution of the Nd moments (see the text). (b) The magnetization of $NdCr_3(BO_3)_4$ at $T=2$ K. The linear dependence shown by a dashed line is an approximation for the low-field data.

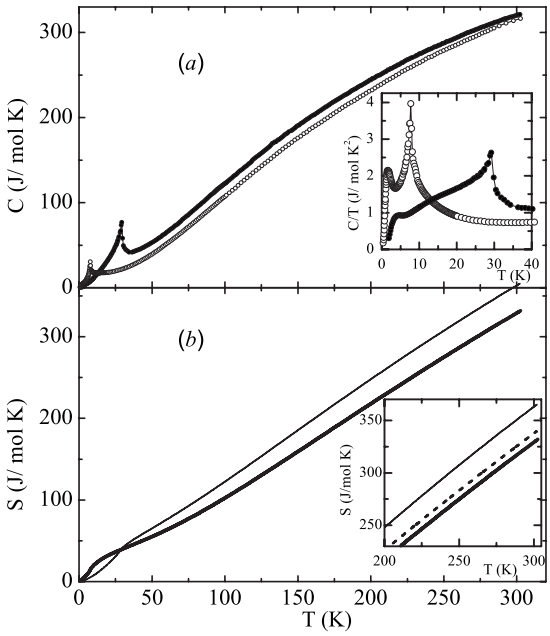

FIG. 2. (a) Temperature dependence of the specific heat $C(T)$ of $NdCr_3(BO_3)_4$ (closed circles) and of $NdFe_3(BO_3)_4$ (open circles). The inset shows the $\frac{C(T)}{T}$ dependence in the temperature range below 40 K. (b) Temperature dependence of the entropy $S(T)$ calculated by means of Eq. (1) for $NdCr_3(BO_3)_4$ (thick line) and for $NdFe_3(BO_3)_4$ (thin line). The inset presents the $S(T)$ dependences in the temperature range 200–300 K. The dashed line displays the renormalized $\tilde{S}(T_2)$ dependence calculated by means of Eq. (A5) taking into account Eq. (A2). The difference along the vertical axis between the two lowest parallel lines represents the difference of magnetic entropies released in $NdFe_3(BO_3)_4$ and $NdCr_3(BO_3)_4$ compounds $\Delta S=9\pm2$ J/mol K (see the text and the Appendix).

using a Quantum Design Physical Properties Measurement System (PPMS). Optical absorption spectra in the spectral region 5000–25000 cm^{-1} at a resolution up to 0.2 cm^{-1} were registered by a Fourier-transform spectrometer Bruker IFS 125HR with InSb liquid-nitrogen-cooled detector and Si detector. The sample was in a helium-vapor optical cryostat at a variable (4.2–300 K) temperature stabilized within ±0.1 K.

III. RESULTS

A. Thermodynamic properties

Figure 1 shows the temperature dependence of the magnetic susceptibility $\chi(T)$ in a magnetic field $B=1$ kG. At high temperatures, the magnetic susceptibility obeys the Curie-Weiss law. Fitting the data yields the Weiss temperature $\Theta \approx -26$ K and the effective magnetic moment $\mu_{\text{eff}}=7.8\mu_B$. We mention that the latter can be well explained by considering the magnetic ions in the compound, i.e., Cr^{3+} and Nd^{3+} ions. Assuming their g factors and total moments as $g_{\text{Cr}}=2$, $J_{\text{Cr}}=s=3/2$ for the Cr^{3+} ion and $g_{\text{Nd}}=8/11$, $J_{\text{Nd}}=9/2$ for the Nd^{3+} ion, we obtain the effective magnetic moment $\mu_{\text{eff}}=\sqrt{3\mu_{\text{eff}}(Cr^{3+})^2+\mu_{\text{eff}}(Nd^{3+})^2}\approx 7.6\mu_B$ which is in a good agreement with the experimental data. The negative value of the Curie-Weiss temperature points to a predominance of antiferromagnetic exchange interactions.

At low temperatures, the magnetization data display a broad maximum at ~12 K and a relatively sharp minimum at about 8 K. Below 8 K, the magnetic susceptibility increases upon cooling. In order to characterize the low-temperature phase, the field dependence of magnetization $M(B)$ at $T=2$ K is shown in the inset of Fig. 1. At low fields below 20 kG, the data imply a linear field dependence of the magnetization and a susceptibility of $0.031\mu_B$/kG. At higher fields, the $M(B)$ curve has a concave character pointing to the absence of a ferromagnetic contribution but to a AFM character of the magnetization curve. The magnetic measurements performed on nonoriented crystals do not allow us to draw a more detailed conclusion.

Figure 2 presents the temperature dependence of the specific heat $C(T)$ of $NdCr_3(BO_3)_4$. There is a sharp λ-like anomaly at about 8 K which points to a second-order phase transition. This anomaly coincides with the minimum in the magnetic susceptibility (see Fig. 3) and, most probably, indicates the onset of a long-range magnetic order at this tem-

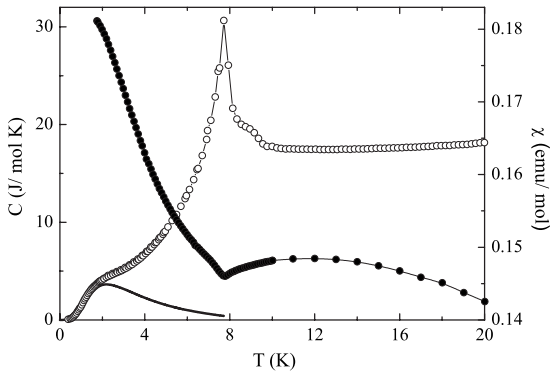

FIG. 3. Temperature dependence of the specific heat and magnetic susceptibility of $NdCr_3(BO_3)_4$ below 24 K. Solid line represents Schottky anomaly calculated by means of Eq. (5).

perature. This assumption is corroborated by the comparison with specific-heat data of the isostructural compound $NdFe_3(BO_3)_4$ (Ref. 17) which are presented in Fig. 2. The latter compound is known to order antiferromagnetically at 29 K (Refs. 17 and 18) which manifests itself by a λ-type anomaly at this temperature.

In addition to the pronounced anomaly at T_N, there is also a small bump at low temperature which implies additional entropy changes in terms of so-called Schottky contributions to the specific heat. This kind of anomaly is well known for compounds with rare-earth ions and can be attributed to the depopulation of an excited energy level of a rare-earth ion.

We emphasize the absence of any other specific heat anomaly and thus of any additional phase transition in $NdCr_3(BO_3)_4$ below 300 K. In particular, this observation suggests the absence of a structural transition. We hence conclude that the space group $R32$ established by the x-ray analysis at room temperature is realized at low temperature, i.e., in the spin-ordered phase, too. This observation agrees to the finding for the isostructural iron borates $RFe_3(BO_3)_4$, R = Y, Er-Eu, where a first-order structural phase transition is only observed for small rare-earth ions.[7,10,19,20] To be specific, the transition into the less symmetric low-temperature structure with the space group $P3_121$ is suppressed by increasing the ionic radius of the R^{3+} ion, from 350 K for the Y compound[10] to 88 K for the Eu compound.[7] For the R^{3+} ions larger than Eu^{3+} (for Nd^{3+}, in particular) rare-earth iron borates possess the $R32$ structure down to the lowest measured temperatures.[7,10] This fact is reflected by the absence of an additional anomaly in the specific heat of $NdFe_3(BO_3)_4$ up to 300 K which is similar to the data for the compound under study in this paper.

B. Optical spectroscopy

The optical absorption spectra of $NdCr_3(BO_3)_4$ exhibit the broad $^4T_2$ and $^4T_1$ bands of Cr^{3+} centered at 16 700 and 22 700 cm^{-1}, respectively.[16] Because of these absorption bands, our samples were completely opaque above 14 000 cm^{-1}. Relatively narrow absorption bands of Nd^{3+} are observed at about 6000, 12 500, and 13 400 cm^{-1}. They are due to f-f optical transitions between the Stark sublevels of

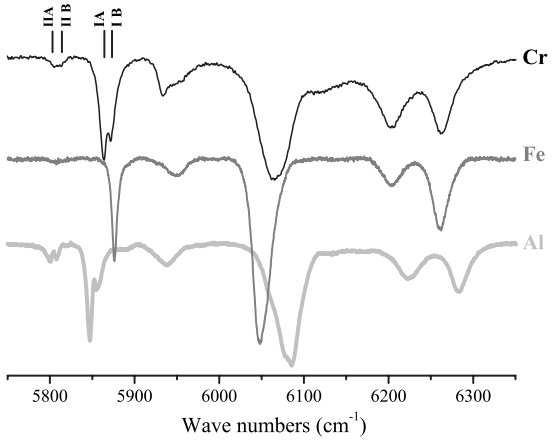

FIG. 4. Transmission spectra of $NdCr_3(BO_3)_4$ (thin black line), $NdFe_3(BO_3)_4$ (thick black line), and $Nd_{0.1}Gd_{0.9}Al_3(BO_3)_4$ (gray line) at 50 K in the region of the $^4I_{9/2} \rightarrow {}^4I_{15/2}$ optical transition in Nd^{3+}.

the ground level $^4I_{9/2}$ of the Nd^{3+} ion and the Stark sublevels of the excited levels $^4I_{15/2}$, $^4F_{5/2}+{}^2H_{9/2}$, and $^4F_{7/2}+{}^4S_{3/2}$, respectively. An energy level of the Nd^{3+} ion with the total momentum J is split into $(J+1/2)$ Kramers doublets by the crystal field of any symmetry lower than a cubic one (the remaining Kramers degeneracy cannot be lifted by any perturbation but the magnetic field).

Figure 4 displays the $^4I_{9/2} \rightarrow {}^4I_{15/2}$ optical multiplet in $NdCr_3(BO_3)_4$ (it was the only multiplet with nonsaturated lines in the spectra of our samples) and, for comparison, in the two other neodymium compounds having the huntite-type $R32$ crystal structure, $NdFe_3(BO_3)_4$ and $Nd_{0.1}Gd_{0.9}Al_3(BO_3)_4$. In this structure, Nd^{3+} ions occupy a single trigonal-symmetry position (point group D_3). The crystal field splits the levels $^4I_{9/2}$ and $^4I_{15/2}$ into five and, respectively, eight Stark sublevels (see Fig. 5). At room temperature, all the Stark sublevels of the ground level $^4I_{9/2}$ are more or less populated and the $^4I_{9/2} \rightarrow {}^4I_{15/2}$ optical multiplet consists of many superimposed broad lines. Spectral lines narrow gradually with decreasing the temperature from

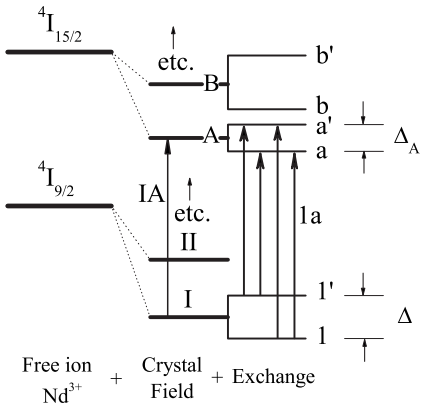

FIG. 5. Stark and exchange splittings of energy levels of the free Nd^{3+} ion caused by the crystal field and magnetic interactions in a magnetically ordered state, respectively.

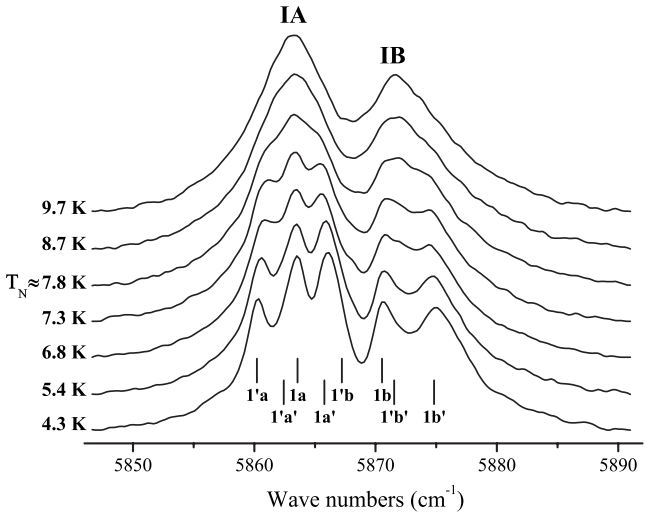

FIG. 6. Absorption line due to the optical transition from the ground level of $NdCr_3(BO_3)_4$ to the two lowest Stark sublevels of the $^4I_{15/2}$ level, at different temperatures. Components of the lines split in a magnetically ordered state are labeled according to the scheme of Fig. 5.

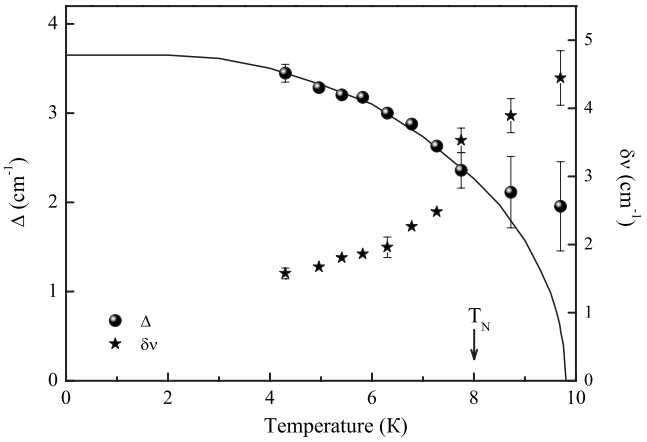

FIG. 7. Temperature dependence of the ground-state splitting Δ (circles) and the linewidth $\delta\nu$ (stars) for $NdCr_3(BO_3)_4$. Solid line is the result of fitting with the values $g_{Nd}=2.385$ and $\lambda_{Cr\text{-}Cr}=29.4$ kG/μ_B, $\lambda_{Nd\text{-}Cr}=3.3$ kG/μ_B for the magnetic g factor of the Nd^{3+} ground state and the molecular-field constants, respectively [see Eqs. (2)–(4) and the text].

300 K to about 10 K and several lines disappear. This freezing out of several lines corresponds to an emptying of excited Stark sublevels of the ground level $^4I_{9/2}$. The lines that remain at low temperatures are due to transitions from the ground state to the Stark sublevels of the exited level $^4I_{15/2}$ and reflect the Stark structure of this level (we should note that the lowest-frequency doublet IIA-IIB in Fig. 4 corresponds to the transition from the first excited Stark level situated at 57 cm^{-1} and vanish at lower temperatures). As it is evident from Fig. 4, the Stark structures are very similar for all three compounds, which suggests a similarity of crystal fields acting upon Nd^{3+} ions and, hence, a similarity of their crystal structure, in agreement with x-ray and specific heat data. The total Stark splitting as well as the splitting between the two lowest-frequency Stark sublevels A and B grows when the ionic radius r of the M^{3+} ion in $NdM_3(BO_3)_4$ diminishes from $r=0.66$ Å for Fe^{3+} via $r=0.62$ Å for Cr^{3+} to $r=0.53$ Å for Al^{3+}, in accordance with growing crystal-field strength. It was not possible to determine the whole Stark structure of the ground level $^4I_{9/2}$ from our limited spectral data on $NdCr_3(BO_3)_4$ but it is reasonable to assume that the energies of these Stark levels are close to those found earlier for $NdFe_3(BO_3)_4$, namely, 0, 65, 141, 221, and 309 cm^{-1}.[21]

Figure 6 shows two lowest-frequency lines IA and IB of the discussed spectral multiplet in $NdCr_3(BO_3)_4$ at several temperatures below 10 K. The growing splitting of the lines into several components and narrowing of spectral lines with decreasing the temperature below 8 K is clearly observed. Each of the lines IA and IB originates from the optical transition between two Kramers doublets of the Nd^{3+} ion. The observed splitting of spectral lines in the $^4I_{9/2} \rightarrow {}^4I_{15/2}$ optical multiplet of $NdCr_3(BO_3)_4$ manifests the presence of an internal magnetic field, which supports the assumption of long-range spin order. A spectral line splits, in general, into four components, as shown in Fig. 5. Two lowest-frequency ones freeze out with decreasing temperature due to an emptying of the upper component of the split ground Kramers doublet of Nd^{3+}. The analysis of the line splitting allows to estimate the splitting of the ground-state Kramers doublet of the Nd^{3+} ion. The temperature dependences of the ground-state splitting $\Delta(T)$ and of the linewidth $\delta\nu(T)$ are shown in Fig. 7. The point of inflection at $T_N \approx 8$ K in the $\Delta(T)$ and $\delta\nu(T)$ dependences corresponds to the temperature of magnetic ordering (see, e.g., Ref. 22) which corroborates the assumption that the specific heat anomaly is due to long-lange spin-ordering in the Cr^{3+} subsystem. A "tail" of residual splittings at $T > T_N$ indicates short-range magnetic order.[22] The spectroscopic data hence demonstrate that the magnetic ordering occurs as a second-order phase transition at $T_N=8\pm0.5$ K, which is in good agreement with the magnetization and the specific heat measurements.

IV. DISCUSSION

To conclude the experimental data and their analysis, we strongly evidence from the spectroscopic and specific heat measurements that (i) the crystal structure of $NdCr_3(BO_3)_4$ down to the lowest temperatures is described by the trigonal space group $R32$ and (ii) the long-range spontaneous magnetic order establishes at $T_N=8$ K. At the same temperature, there is a kink in the magnetic susceptibility curve. The magnetization curve $M(B)$ [cf. Fig. 1(b)] proves the magnetic order to be antiferromagnetic since $\partial M/\partial B$ is constant in low fields and *increases* in higher fields. A spin gap, i.e., a nonmagnetic ground state, or a spin level crossing which might yield the observed concave magnetization curve, too, is excluded by the specific heat and $M(T)$ data.[23,24] We mention that the observation of antiferromagnetic correlations at high temperatures which is probed by the negative value of the Weiss temperature of $\Theta \approx -26$ K qualitatively agrees to the observed antiferromagnetic ordering. However, in contrast to

a simple AFM behavior we find that the magnetization increases upon cooling below $T_N=8$ K. This observation indicates that not both magnetic subsystems, i.e., the chromium and the neodymium one, undergo the magnetic ordering phase transition. Instead, this behavior can be explained, as it has been done for other *f-d* compounds containing both 3*d*-(like chromium) and 4*f*-(like neodymium) magnetic ions (see, e.g., Refs. 25 and 26), by assuming that the antiferromagnetic ordering occurs only in the Cr subsystem while the Nd subsystem remains paramagnetic down to the lowest temperatures and being polarized by the ordered chromium subsystem [a semiqualitative description of the $\chi(T)$ curve for $NdCr_3(BO_3)_4$ will be given below]. This is a rather general situation for the *f-d* compounds. It is based on the relative strength of interactions between different magnetic ions in these mixed magnetic dielectrics. Usually the strongest magnetic interactions are those within the 3*d* subsystem, followed by the *d-f* ones, while the *f-f* interactions are negligible.[22] This latter statement is especially true in the case of the rare-earth borates $RM_3(BO_3)_4$ where the RO_6 polyhedra in the crystal structure are well isolated having no common oxygen atoms.

Further support to the scenario of a magnetic ordering within the chromium subsystem comes from the analysis of the entropy

$$S(T) = \int_0^T \frac{C(T)}{T} dT \tag{1}$$

which is presented in Fig. 2(b) for $NdCr_3(BO_3)_4$ and $NdFe_3(BO_3)_4$. The data show a similar temperature dependence of the entropy for both compounds, i.e., the chromium and the iron one. While it is impossible to separate the lattice contributions from those of the two magnetic subsystems, valuable information can be drawn from comparing the two data sets. The data suggest that, at temperatures above 150 K, the observed entropy changes are due to the lattice degrees of freedom and due to the term $S_{Nd}(T)$ arising from the populated Stark sublevels of the Nd^{3+} ground level $^4I_{9/2}$ while the full magnetic entropy has already been achieved. This assumption is strongly supported by the fact that at high temperatures the $C(T)$ dependencies are identical if a renormalization is performed which takes into account the different ionic masses and lattice force constants (see the Appendix). In addition, the magnetic entropies of $NdFe_3(BO_3)_4$ and of $NdCr_3(BO_3)_4$ in the temperature range 150–300 K differ by a constant value of $\Delta S=9\pm2$ J/mol K. This value found by using Eq. (A4) explained in the Appendix is in good agreement with the theoretical estimate for magnetically ordered systems $\Delta S=3R[\ln(2^*5/2+1) - \ln(2^*3/2+1)]=10.1$ J/mol K which one expects from the different values of the transition-metal spins, i.e., $s_{Fe}=5/2$ for Fe^{3+} and $s_{Cr}=3/2$ for Cr^{3+} ($R=8.31$ J/mol K is the gas constant).

In the framework of the molecular-field approximation, the interaction between Nd^{3+} ions and the ordered Cr^{3+} magnetic subsystem can be substituted by an effective ("molecular") magnetic field

$$B_{Nd}(T) = 3\lambda_{Nd\text{-}Cr} M(T), \tag{2}$$

where $\lambda_{Nd\text{-}Cr}$ is the molecular-field constant of the Nd-Cr interaction. The factor 3 in Eq. (2) reflects the fact that there are three Cr atoms for every Nd atom in the formula unit, while the magnetization of the Cr subsystem is normalized per site. In this approximation, the observed Nd^{3+} ground Kramers doublet splitting Δ can be considered as Zeeman splitting,

$$\Delta(T) = g_{Nd}\mu_B B_{Nd}(T). \tag{3}$$

Here, g_{Nd} is the spectroscopic *g* factor for the Nd^{3+} ground Kramers doublet while at the very beginning of Sec. III A we have used the so-called Lande *g* factor for the Nd^{3+} ground multiplet $^4I_{9/2}$. The matter is that at low temperatures only the ground Kramers doublet of Nd^{3+} is populated while at high temperatures we must average over all the crystal-field sublevels of the Nd^{3+} ground multiplet $^4I_{9/2}$. Taking $g_{Nd}=2.385$, the same as for $NdFe_3(BO_3)_4$ (Ref. 26) (which is justified by a similarity of crystal fields in both compounds), and the experimental value $\Delta=3.7$ cm^{-1} we obtain $B_{Nd}\approx35$ kG for the lowest temperature. Substituting this value of B_{Nd} and the maximum value of the Cr^{3+} magnetic moment $M=g_{Cr}s\mu_B=3\mu_B$ in Eq. (2) gives $\lambda_{Nd\text{-}Cr}=3.9$ kG/μ_B for the molecular-field constant of the Nd-Cr interaction.

The temperature dependence of the Nd^{3+} ground-state splitting $\Delta(T)$ is reasonably well proportional to the $M(T)$ dependence deduced from the molecular-field theory as applied to the Cr^{3+} magnetic subsystem (see Fig. 7). The solid curve in Fig. 7 was found from the well-known equation of a simple mean-field theory,

$$M = g_{Cr}s\mu_B B_{3/2}\left(\frac{g_{Cr}\mu_B s\lambda_{Cr\text{-}Cr}M}{kT}\right). \tag{4}$$

Here, μ_B is the Bohr magneton, $B_{3/2}(y)$ is the Brillouin function for the Cr^{3+} ion, and $\lambda_{Cr\text{-}Cr}$ is the molecular-field constant relevant to the chromium magnetic subsystem. The fitting of ground-state splitting $\Delta(T)$ gives the estimation of the molecular-field constant $\lambda_{Cr\text{-}Cr}=29.4$ kG/μ_B of the Cr-Cr interaction. The $\Delta(T)$ dependence is described well up to 7.5 K by means of $M(T)$ derived from Eq. (4). However, this approximation gives an overestimated value of the transition temperature T_N. At least two reasons for such a discrepancy can be mentioned. First, the mean-field theory is not valid for temperatures close to the phase transition temperature, because it does not take into account fluctuation phenomena. Second, and probably, more important, a very simple approximation with only one molecular-field constant λ was used to describe the behavior of the chromium subsystem while interactions within this subsystem containing Cr-O-Cr chains are essentially anisotropic.

Depopulation of the upper component of the Nd^{3+} ground Kramers doublet split in the effective magnetic field created by the magnetically ordered chromium subsystem results in the Schottky contribution to the specific heat. The splitting $\Delta(T)$, determined from the optical data, gives us a possibility to estimate the contribution of the Nd subsystem into the specific heat, according to the following relation:[27]

$$C_{\mathrm{Nd}}(T) = R\left(\frac{\Delta(T)}{kT}\right)^2 \frac{\exp(\Delta(T)/kT)}{\{\exp[\Delta(T)/kT]+1\}^2}. \quad (5)$$

Applying Eq. (5) to calculate the temperature dependence of the Schottky contribution (cf. the solid line in Fig. 3) yields a good description of the experimental data so that the bump in the specific heat data can unambiguously be attributed to the Schottky anomaly.

The Schottky-like anomaly should be also visible in the temperature dependence of the magnetic susceptibility in Fig. 1. Contrary to the case of the heat capacity, its shape should depend on the specific arrangement of the ordered magnetic moments of chromium. It has been shown earlier that for the iron borates $R\mathrm{Fe}_3(\mathrm{BO}_3)_4$ a specific arrangement of the magnetic moments in the magnetically ordered phase is imposed by the ground-state single-ion anisotropy of a particular rare-earth R^{3+} ion and is either of the easy-axis or of the easy-plane type.[11,26,28] In particular, in $\mathrm{NdFe}_3(\mathrm{BO}_3)_4$, the Fe magnetic moments form a collinear antiferromagnetic (AF) structure along one of the C_2 axes in the *ab* plane of the crystal, so that three types of domains exist corresponding to the three equivalent C_2 axes.[29] It is reasonable to assume that the magnetic structure of the rare-earth chromium borates is of either the easy-axis or of the easy-plane type, too. The supposition that the magnetic moments of both Cr and Nd ions are aligned along the *c* axis of the $\mathrm{NdCr}_3(\mathrm{BO}_3)_4$ crystal would result in the Schottky-like anomaly at about 3 K. Moreover, the total magnetic susceptibility would quickly decrease upon cooling below 3 K because of both the chromium and neodymium subsystem even for polycrystalline samples. This is not observed experimentally. On the contrary, when assuming that three types of AF domains with the directions of Cr magnetic moments along the C_2 axes in the basal plane are statistically distributed, we obtain the Schottky-like Nd contribution $\chi_{\mathrm{Nd}}(T)$ to the magnetic susceptibility of a polycrystalline sample with a maximum at about 1.8 K. This conclusion follows from our calculation in the framework of the above-mentioned model, according to the formula

$$\chi_{\mathrm{Nd}} = \frac{N_A g_\perp^2 \mu_B^2}{2kT}\left(\frac{2}{3}\frac{\exp\left(\frac{\Delta(T)}{kT}\right)+0.5\frac{kT}{\Delta(T)}\left[\exp\left(\frac{\Delta(T)}{kT}\right)-1\right]}{\left[\exp\left(\frac{\Delta(T)}{kT}\right)+1\right]^2} + \frac{1}{3}\frac{g_\parallel^2 T}{g_\perp^2 \Delta(T)}\frac{\exp\left(\frac{g_\perp \Delta(T)}{g_\parallel kT}\right)-1}{\exp\left(\frac{g_\perp \Delta(T)}{g_\parallel kT}\right)+1}\right), \quad (6)$$

with $g_\perp = 2.385$ and $g_\parallel = 1.376$, as taken from Ref. 26 (here again, $g_\perp$ and $g_\parallel$ are the transversal and, respectively, the longitudinal *g* factors of the Nd^{3+} ground Kramers doublet).

The inset of Fig. 1(a) displays the results of calculation for $\chi_{\mathrm{Nd}}(T)$ in the cases of easy axis (dashed line) and easy plane, as discussed above (solid line), antiferromagnet, compared to the low-temperature part of the experimentally measured total magnetic susceptibility of a polycrystalline sample (open circles). The maximum at 1.8 K in the calculated $\chi_{\mathrm{Nd}}(T)$ dependence is in good agreement with the experimental points near the lowest in our SQUID experimentally accessible temperature of 1.75 K. The rapid increase of $\chi_{\mathrm{Nd}}(T)$ below T_N is partly compensated by the decrease of the magnetic susceptibility of the ordered chromium subsystem. Thus, an increase of the measured $\chi(T)$ dependence at $T < T_N$ is in agreement with the contribution of the paramagnetic Nd subsystem polarized by the Cr magnetic moments ordered into the easy-plane magnetic structure. Whether a decrease of $\chi(T)$ just below T_N is observed [as, e.g., in $\mathrm{NdFe}_3(\mathrm{BO}_3)_4$ (Ref. 26)] or not [as, e.g., in $\mathrm{Nd}_2\mathrm{BaNiO}_5$ (Refs. 30 and 31)] depends on the relative contributions of the *d*- and *f*-magnetic subsystems.

An essential structural feature of $\mathrm{NdCr}_3(\mathrm{BO}_3)_4$ is the presence of chromium chains. The broad maximum at 12 K in the $\chi(T)$ dependence is possibly caused by the low dimensionality of the chromium magnetic system.[32] In Ref. 33, the following formula has been proposed to model the magnetic susceptibility of the Heisenberg antiferromagnetic spin chain with $s = 3/2$:

$$\chi_{\mathrm{Cr}} = \frac{N_A s(s+1) g^2 \mu_B^2}{3kT}\frac{1+u(K)}{1-u(K)}, \quad (7)$$

where

$$u(K) = \coth K - \frac{1}{K},$$

$$K = -\frac{2Js(s+1)}{kT},$$

and *J* is defined as positive for antiferromagnetic coupling inside the chain, e.g., $H_{\mathrm{exch}} = 2J\Sigma_{i>j} s_i s_j$. This function has already been used with success for different spin chains.[34–37] The solid line in Fig. 1 shows the magnetic susceptibility of the $s = 3/2$ spin chain calculated with the value of the intrachain exchange parameter $J/k = 4$ K. This value is a good agreement with the $J/k = 3.8$ K estimated from the molecular-field constant $\lambda_{\mathrm{Cr\text{-}Cr}}$. One can see that the broad maximum observed in the experimental $\chi(T)$ dependence is reproduced rather well. Besides, a noticeable deviation of the magnetic susceptibility from the Curie-Weiss law below ~ 50 K $= 6T_N$ and a pronounced "tail" of residual splitting of spectral lines at $T > T_N$ suggest that short-range spin correlations remain at temperatures well above T_N, which is a characteristic feature of low-dimensional systems (see, e.g., Refs. 22 and 32).

V. CONCLUSIONS

We have undertaken the investigation of thermal and magnetic properties and the high-resolution spectroscopic study of the $\mathrm{NdCr}_3(\mathrm{BO}_3)_4$ compound in a broad range of temperatures. The totality of x-ray diffraction, specific heat, and optical data on $\mathrm{NdCr}_3(\mathrm{BO}_3)_4$ has revealed the huntite-type crystal structure with the space group *R*32 for this compound in the whole range of the investigated temperatures.

The analysis of thermal, magnetic, and optical properties has shown that $NdCr_3(BO_3)_4$ undergoes a second-order antiferromagnetic ordering phase transition at $T_N=8$ K. The magnetic phase transition occurs only in the chromium subsystem while the neodymium subsystem remains paramagnetic down to the lowest temperatures being polarized by the interaction with the ordered Cr magnetic subsystem. It was shown that this interaction can be treated in the molecular-field approximation with the molecular-field constants $\lambda_{Nd\text{-}Cr}=3.9$ kG/μ_B and $\lambda_{Cr\text{-}Cr}=29.4$ kG/μ_B. The observed splitting $\Delta(T)=3.7$ cm^{-1} of the ground-state Kramers doublet of Nd^{3+} has given the following estimate of the strength of this field at 1.8 K, $B\approx 35$ kG. We have demonstrated that the Schottky anomaly in specific heat at low temperatures is well reproduced when taking the $\Delta(T)$ dependence found from our optical measurements. The analysis of magnetic susceptibility data allowed one to suggest the antiferromagnetic ordering of the easy-plane type. Several experimental manifestations of low dimensionality of the title compound were mentioned.

ACKNOWLEDGMENTS

This work was supported by the Russian Foundation for Basic Research, Grants Nos. 07-02-01185, 04-05-64709, and 05-05-08021 and by the Russian Academy of Sciences under the Programs for Basic Research. The authors acknowledge funding by the Deutsche Forschungsgemeinschaft through Contracts Nos. HE-3439/6 and 436 RUS 113/864/0-1.

APPENDIX

In the present work, we use the specific heat data on the isostructural compound $NdFe_3(BO_3)_4$ (Ref. 17) for estimating the difference of magnetic entropies released in $NdFe_3(BO_3)_4$ and $NdCr_3(BO_3)_4$. We find empirical constants a and b, such that the curves $C(T)$ for $NdFe_3(BO_3)_4$ and $C(aT+bT^2)$ for $NdCr_3(BO_3)_4$ coincide in the high-temperature paramagnetic range ($\sim$150–300 K) where we expect purely lattice specific heat. In other words, we write [here and below, subscripts 1 and 2 correspond to $NdFe_3(BO_3)_4$ and $NdCr_3(BO_3)_4$ compounds, respectively]

$$C_{\mathrm{lat1}}(T_1)=C_{\mathrm{lat2}}(T_2), \tag{A1}$$

$$T_2=T_1(a+bT_1), \tag{A2}$$

and find $a=1.13$, $b=-3.3\times10^{-4}$ K^{-1}. In the first approximation, the parameter a is the ratio of "Debye temperatures" for chromium and iron compounds, $a=\frac{\theta_2}{\theta_1}=1.13$, while the parameter b reflects the possible difference in the shape of phonon and in the positions of Nd^{3+} crystal-field levels in these compounds. The entropy calculated up to T_2 in $NdCr_3(BO_3)_4$ is

$$\begin{aligned} S_2(T_2)&=\int_0^{T_2}\frac{C_{\mathrm{lat2}}(T)}{T}dT+S_{\mathrm{mag2}} \\ &=\int_0^{T_1}\frac{C_{\mathrm{lat1}}(T')}{T'}\frac{(a+2bT')}{(a+bT')}dT'+S_{\mathrm{mag2}}. \end{aligned} \tag{A3}$$

Here, we use the substitution $T=T'(a+bT')$ and take into account Eq. (A1). After simple mathematical transformations we obtain that in the high-temperature range the difference of magnetic entropies released in $NdFe_3(BO_3)_4$ and $NdCr_3(BO_3)_4$ compounds reads as follows:

$$\Delta S=S_{\mathrm{mag}}^{\mathrm{NdFe}}-S_{\mathrm{mag}}^{\mathrm{NdCr}}=S_{\mathrm{mag1}}-S_{\mathrm{mag2}}=\tilde{S}(T_1)-S_2(T_2), \tag{A4}$$

$$\tilde{S}(T_1)=S_1(T_1)+S_1(T_1)\frac{bT}{a+bT}-\int_0^{T_1}S_1(T)\frac{ab}{(a+bT)^2}dT, \tag{A5}$$

where temperatures T_1 and T_2 are connected by Eq. (A2).

*eapopova@yahoo.com

[1] N. I. Leonyuk and L. I. Leonyuk, Prog. Cryst. Growth Charact. Mater. **31**, 179 (1995).
[2] A. A. Filimonov, N. I. Leonyuk, L. B. Meissner, T. I. Timchenko, I. S. Rez, Krist. Tech. **9**, 63 (1974).
[3] L. M. Dorozhkin, I. I. Kuratev, N. I. Leonyuk, T. I. Timchenko, and A. V. Shestakov, Pis'ma Zh. Tekh. Fiz. **7**, 1297 (1981).
[4] D. Jaque, J. Alloys Compd. **323-324**, 204 (2001).
[5] M. Huang, Y. Chen, X. Chen, Y. Huang, and Z. Luo, Opt. Commun. **208**, 163 (2002).
[6] X. Chen, Z. Luo, D. Jaque, J. J. Romero, J. G. Sole, Y. Huang, A. Jiang, and C. Tu, J. Phys.: Condens. Matter **13**, 1171 (2001).
[7] Y. Hinatsu, Y. Doi, K. Ito, M. Wakeshima, and A. Alemi, J. Solid State Chem. **172**, 438 (2003).
[8] A. D. Balaev, L. N. Bezmaternykh, I. A. Gudim, V. L. Temerov, S. G. Ovchinnikov, and S. A. Kharlamova, J. Magn. Magn. Mater. **258-259**, 532 (2003).
[9] R. Z. Levitin, E. A. Popova, R. M. Chtsherbov, A. N. Vasiliev, M. N. Popova, E. P. Chukalina, S. A. Klimin, P. H. M. van Loosdrecht, D. Fausti, and L. N. Bezmaternykh, JETP Lett. **79**, 531 (2004).
[10] D. Fausti, A. A. Nugroho, P. H. M. van Loosdrecht, S. A. Klimin, M. N. Popova, and L. N. Bezmaternykh, Phys. Rev. B **74**, 024403 (2006).
[11] M. N. Popova, E. P. Chukalina, T. N. Stanislavchuk, and L. N. Bezmaternykh, Bull. Russ. Acad. Sci. Phys. **70**, N11 (2006).
[12] A. K. Zvezdin, S. S. Krotov, A. M. Kadomtseva, G. P. Vorob'ev, Yu. F. Popov, A. P. Pyatakov, L. N. Bezmaternykh, and E. A. Popova, JETP Lett. **81**, 272 (2005).
[13] A. K. Zvezdin, A. M. Kadomtseva, S. S. Krotov, A. P. Pyatakov, Yu. F. Popov, and G. P. Vorob'ev, J. Magn. Magn. Mater. **300** 224 (2006).
[14] F. Yen, B. Lorenz, Y. Y. Sun, C. W. Chu, L. N. Bezmaternykh, and A. N. Vasiliev, Phys. Rev. B **73**, 054435 (2006).

[15] A. D. Mills, Inorg. Chem. **1**, 960 (1962).
[16] H.-D. Hattendorff, G. Huber, and H. G. Danielmeyer, J. Phys. C **11**, 2399 (1978).
[17] N. Tristan, R. Klingeler, C. Hess, B. Büchner, E. Popova, I. A. Gudim, and L. N. Bezmaternykh, J. Magn. Magn. Mater. **316**, e621 (2007).
[18] E. P. Chukalina, D. Y. Kuritsin, M. N. Popova, L. N. Bezmaternykh, S. A. Kharlamova, and V. L. Temerov, Phys. Lett. A **322**, 239 (2004).
[19] S. A. Klimin, D. Fausti, A. Meetsma, L. N. Bezmaternykh, P. H. M. van Loosdrecht, and T. T. M. Palstra, Acta Crystallogr., Sect. B: Struct. Sci. **61**, 481 (2005).
[20] A. N. Vasiliev, E. A. Popova, I. A. Gugim, L. N. Bezmaternykh, and Z. Hiroi, J. Magn. Magn. Mater. **300**, e382 (2006).
[21] E. P. Chukalina (unpublished).
[22] M. N. Popova, J. Alloys Compd. **275-277**, 142 (1998).
[23] R. Klingeler, B. Buchner, K.-Y. Choi, V. Kataev, U. Ammerahl, A. Revcolevschi, and J. Schnack, Phys. Rev. B **73**, 014426 (2006).
[24] C. Golze, A. Alfonsov, R. Klingeler, B. Buchner, V. Kataev, C. Mennerich, H.-H. Klauss, M. Goiran, J.-M. Broto, H. Rakoto, S. Demeshko, G. Leibeling, and F. Meyer, Phys. Rev. B **73**, 224403 (2006).
[25] M. N. Popova, S. A. Klimin, E. P. Chukalina, B. Z. Malkin, R. Z. Levitin, B. V. Mill, and E. Antic-Fidancev, Phys. Rev. B **68**, 155103 (2003).
[26] M. N. Popova, E. P. Chukalina, T. N. Stanislavchuk, B. Z. Malkin, E. Antic-Fidancev, E. A. Popova, L. N. Bezmaternykh, and V. L. Temerov, Phys. Rev. B **75**, 224435 (2007).
[27] K. N. R. Taylor and M. I. Darby, *Physics of Rare Earth Solids* (Chapman and Hall, London, 1972).
[28] E. A. Popova, D. V. Volkov, A. N. Vasiliev, A. A. Demidov, N. P. Kolmakova, I. A. Gudim, L. N. Bezmaternykh, N. Tristan, Yu. Skourski, B. Büchner, C. Hess, and R. Klingeler, Phys. Rev. B **75**, 224413 (2007).
[29] P. Fischer, V. Pomjakushin, D. Sheptyakov, L. Keller, M. Janoschek, B. Roessli, J. Schefer, G. Petrakovskii, L. Bezmaternikh, V. Temerov, and D. Velikanov, J. Phys.: Condens. Matter **18**, 7975 (2006).
[30] G. G. Chepurko, Z. A. Kazei, D. A. Kudrjavtsev, R. Z. Levitin, B. V. Mill, M. N. Popova, and V. V. Snegirev, Phys. Lett. A **157**, 81 (1991).
[31] E. García-Matres, J. L. García-Munos, J. L. Martínez, and J. Rodríguez-Carvajal, J. Magn. Magn. Mater. **149**, 363 (1995).
[32] L. J. de Jongh and A. R. Miedema, Adv. Phys. **50**, 947 (2001).
[33] G. R. Wagner and S. A. Friedberg, Phys. Lett. **9**, 11 (1964).
[34] I. E. Grey and H. Steinfink, Inorg. Chem. **10**, 691 (1971).
[35] N. Nakayama, K. Kosuge, S. Kachi, T. Shinjo, and T. Takada, J. Solid State Chem. **33**, 351 (1980).
[36] R. Dingle, M. E. Lines, and S. L. Holt, Phys. Rev. **187**, 643 (1969).
[37] Andrew D. J. Barnes, Thomas Baikie, Vincent Hardy, Marie-Bernadette Lepetit, Antoine Maignan, Nigel A. Young, and M. Grazia Francesconi, J. Mater. Chem. **16**, 3489 (2006).